

A New Coarse-Grained Force Field for Membrane–Peptide Simulations

Zhe Wu, Qiang Cui,* and Arun Yethiraj*

Theoretical Chemistry Institute and Department of Chemistry, University of Wisconsin, Madison, 1101 University Avenue, Madison, Wisconsin 53706, United States

 Supporting Information

ABSTRACT: We present a new coarse-grained (CG) model for simulations of lipids and peptides. The model follows the same topology and parametrization strategy as the MARTINI force field but is based on our recently developed big multipole water (BMW) model for water (*J. Phys. Chem. B* **2010**, *114*, 10524–10529). The new BMW-MARTINI force field reproduces many fundamental membrane properties and also yields improved energetics (when compared to the original MARTINI force-field) for the interactions between charged amino acids with lipid membranes, especially at the membrane–water interface. A stable attachment of cationic peptides (e.g., Arg₈) to the membrane surface is predicted, consistent with experiment and in contrast to the MARTINI model. The model predicts electroporation when there is a charge imbalance across the lipid bilayer, an improvement over the original MARTINI. Moreover, the pore formed during electroporation is toroidal in nature, similar to the prediction of atomistic simulations but distinct from results of polarizable MARTINI for small charge imbalances. The simulations emphasize the importance of a reasonable description of the electrostatic properties of water in CG simulations. The BMW-MARTINI model is particularly suitable for describing interactions between highly charged peptides with lipid membranes, which is crucial to the study of antimicrobial peptides, cell penetrating peptides, and other proteins/peptides involved in the remodeling of biomembranes.

I. INTRODUCTION

Many biological processes that occur at the cellular membrane involve lipid membrane deformations at many length scales,^{1,2} which are either triggered or facilitated by small peptides³ or complex protein machineries.^{4,5} To effectively complement experimental studies of these processes, it is important to develop computational models that are capable of describing membrane deformations as well as interactions between the membrane and peptides/proteins. The latter requirement highlights the importance of developing particle-based coarse-grained (CG) models for membrane systems, which are particularly useful for phenomena that occur on length and time scales too large for atomistic simulations but where continuum mechanical models^{1,6–8} are not appropriate. In this paper we report a new CG model for lipids and peptides that is based on an accurate CG model for water developed in our groups.

The past decade has seen a flurry of activity in the development of CG models for biomolecules and lipids.^{9–13} By grouping several atoms into a single unit, thus decreasing computational cost, CG models have proven valuable in many simulation studies of biomembranes and their interactions with peptides and proteins.¹² For example, the MARTINI force field^{14,15} has been successfully applied to study lipid vesicle formation and fusion,^{16–19} lipid phase transformation,²⁰ structure and dynamics of lipid bilayers and monolayers,^{14,15,21} and effects of various molecules (e.g., cholesterol, proteins) on the shape and phase behaviors of complex membranes.^{22–25} Solvent-free CG models for membranes have also been proposed and found useful in a number of studies,^{26–28} although transferable protein models that are compatible with these membrane models have not yet been reported to our knowledge.

An important aspect of computational biophysics is the treatment of electrostatic interactions. Driven by a desire for computational efficiency, many CG models choose to remove and/or simplify the treatment of electrostatic interactions. In MARTINI, for example, four water molecules are grouped into a single uncharged unit (bead), and electrostatic interactions between charged beads, which represent either lipid head groups or charged amino acid side chains, are treated with a cutoff scheme and a fairly large dielectric constant ($\epsilon = 15–20$). Although this model can be effective for describing interactions between lipids and nonpolar groups, we expect it to be less appropriate for describing the interaction between lipid membrane and highly charged species, such as cell penetrating peptides and antimicrobial peptides, for which a proper treatment of electrostatics is likely crucial. This is supported by the observation that although MARTINI gives satisfactory results (when compared to atomistic simulations) for the potential of mean force (PMF) for the penetration of nonpolar and polar (neutral or with a small dipole moment) amino acids into lipid bilayers, it incurs large errors for the PMF of charged amino acids, especially positively charged residues.²³

A major source of the error in MARTINI can be attributed to the treatment of water. It has been well established that water molecules near the lipid–water interface make a major contribution to the electrostatic potential profile near that interface.²⁹ Since water molecules are treated as uncharged beads in MARTINI, they do not contribute directly to the electrostatic potential, which is the reason that the calculated interfacial potential at the lipid bilayer–water interface with MARTINI is grossly incorrect

Received: May 1, 2011

Published: September 20, 2011

(MARTINI predicts a value of -0.4 V which may be compared to the experimental estimate^{30,31} of $+0.22$ to 0.28 V and results from atomistic simulations^{32,33} of $+0.4$ to 1.0 V). A natural remedy, therefore, is to include electrostatics for the description of water, which has been recently pursued by several CG models.

In the CG force field of Essex and co-workers,³⁴ water is treated using the soft sticky dipole model of Ichijo and co-workers.³⁵ Although the model has been shown to provide impressive results for the mechanical and electrostatic properties of lipid bilayers, it offers limited computational advantage over atomistic models of water. Moreover, the orientation of lipid head groups in their model is different from atomistic simulations, thus the contributions from different groups to the interfacial potential do not match atomistic results. An improved version of MARTINI, called the polarizable MARTINI force field,³⁶ has been proposed and features a water model with two charged-sites; recent test calculations suggest that the polarizable MARTINI model leads to much improved results for the insertion PMF of charged pentapeptides into a lipid bilayer.³⁷ However, this model still gives qualitatively incorrect results for the interfacial dipole potential (reported as -2 V in ref 36), which suggests that the improved PMF is due in part to error cancellation; it has also been discussed in the literature that the insertion PMF is not a simple function of the interfacial dipole potential.³⁸ More recently, a four-site CG water model (WAT FOUR)³⁹ has been reported. Although the model was constructed to map 5 water molecules into 1 CG unit, the calculated properties (e.g., density) suggested that 1 CG unit effectively reflects 11 water molecules; moreover, the model overestimates the dielectric constant and underestimates the surface tension, thus hampering its applicability to bilayer systems. Finally, a dipolar CG model that represents five water molecules has been proposed very recently;⁴⁰ it reproduces the key properties of water well but has not yet been used to parametrize CG models for other biomolecules.

We have recently developed and reported a new CG model for water, termed as the big multipole water (BMW) model;⁴¹ it features the same four to one mapping as the original MARTINI but includes three explicitly charged sites for each CG unit. Our basic approach starts with using atomistic simulations to characterize the electrostatic properties (multipole moments) and the nonbonded interactions of four water clusters. The results inform us of the appropriate functional forms of electrostatic and nonpolar components of the model; for example, we found it was necessary to describe the nonpolar component with a much softer potential than the commonly used Lennard-Jones (LJ) form. The parameters in the model are then fitted based on comparing experimental and computed properties of water, including bulk density, isothermal compressibility, dielectric permittivity, surface tension, and air–water interface potential. A preliminary combination of the BMW model with MARTINI lipids resulted in a membrane dipole potential that is in good agreement with experimental estimates. Finally, in a recent study,⁴² we have shown that the electrostatic features of the water model also appear important to a proper description of the hydrophobic effect. For the association of two hydrophobic peptides, BMW simulations predict the process as entropy driven, in agreement with atomistic studies,^{43,44} while several nonelectrostatic/dipolar CG water models (MARTINI,¹⁵ polarizable MARTINI³⁶ and the model of Shinoda et al.)⁴⁵ predict the process as enthalpy driven with very small entropic contributions.

In this work, we report our continuing efforts in developing a CG force field for lipids and amino acids with BMW as the basis.

Since the basic topology and parametrization strategy of the force field follow the MARTINI convention, we refer the model as BMW-MARTINI. With a proper treatment of electrostatics but similar limitations in secondary structure descriptions as the original MARTINI, our model in current form is particularly useful for describing the interaction between lipid membrane and highly charged peptide or protein motifs that are either disordered or rigid (i.e., the model is not capable of describing coupled binding/folding processes).

In the following, we first describe how the model is constructed and how the parameters in the model are determined. Next, we present results that illustrate the performance of the BMW-MARTINI model for a fairly broad range of properties concerning lipid membrane and its interaction with amino acids; these include: (i) thermodynamics (free energy and enthalpy–entropy components) of hydration and partitioning between oil–water for basic bead types; (ii) mechanical properties of lipid bilayers and self-assembly of lipids; (iii) potential of mean force for the penetration of amino acid side chains into a lipid bilayer; (iv) behavior of a highly charged peptide (Arg_8) on the surface of a lipid bilayer; and (v) electroporation. Finally, we draw a few conclusions and comment on possible directions for future developments.

II. MODEL AND METHODS

A. Big Multipole Water (BMW). Since the BMW water model forms the basis of our CG force field, we briefly summarize its key features. Four water molecules are mapped into one CG unit with three charged sites (see Figure 1a). Since our atomistic simulations⁴¹ indicated that the distributions of dipole moment and quadrupole moment tensor of four water clusters are similar in bulk water, at the air–water interface, and in salt solutions, we chose the geometry and charges of these sites to reproduce the most probable dipole and quadrupole tensors of four water clusters from atomistic simulations. Nonpolar interactions between sites are represented by a modified Born–Mayer–Huggins (BMH)^{46,47} potential, which features a softer interaction at short distance than the commonly used LJ potential; the soft-core interaction is crucial for avoiding spurious long-range correlations between water molecules. The BMW model is capable of reproducing key properties of bulk water and air–water interface, most notably bulk permittivity, surface tension, and air–water interfacial potential. The BMW is more computationally intensive (by a factor of 6) than the original MARTINI model due to the larger number of sites and the use of particle mesh Ewald (PME) for electrostatics but is nevertheless about two orders of magnitude more computationally efficient than atomistic simulations.

B. Parameterization Strategies. The new force field is parametrized with a strategy that maintains the self-consistency among models for lipids and amino acids. The parametrization is done in a multistage fashion based on carefully monitoring a broad set of properties related to hydration/transfer free energies, lipid bilayer properties, lipid self-assembly, and interaction between amino acids and a lipid bilayer.

First, partition free energies of uncharged bead types between water–air or water–hexadecane are tuned to give the approximate sets of scaling factors for nonpolar interactions. Then, lipid bilayer structural properties and lipid self-assembly phase behaviors are used to fine-tune these scaling factors as well as parameters for charged group (Q)-BMW interactions and the

angle bending force constant for lipid tails. Next, potentials of mean force (PMFs) for the penetration of different amino acids into a dioleoylphosphatidylcholine (DOPC) bilayer are calculated, and the values in the interfacial region are compared with atomistic results⁴⁸ to determine interactions between charged (lipid head groups) and neutral (neutral amino acids) groups. Finally, the insertion PMFs of charged amino acid side chains into a bilayer are used to further refine the interaction between CG beads and BMW water. The initial parametrization of the models is described in this section, and a fine-tuning of the parameters is presented in the Results and Discussion section.

C. Initial Parametrization of Lipid and Amino Acid Potentials. For lipids and amino acids, we follow the same mapping scheme as the MARTINI force field [illustrated in Figure 1b for a dimyristoylphosphatidylcholine (DMPC) molecule].^{15,23} We adopt the same classification scheme for beads: charged (Q), polar (P), nonpolar (N), and apolar (C) for representing similar chemical structures. We also use the same sets of subtypes (with a few changes, see below) to label different levels of effective nonelectrostatic interactions between beads. On the other hand, since the MARTINI force field employs hydration and transfer free energies as the guiding properties for parametrization, changing the underlying water model to BMW requires an extensive reparameterization.

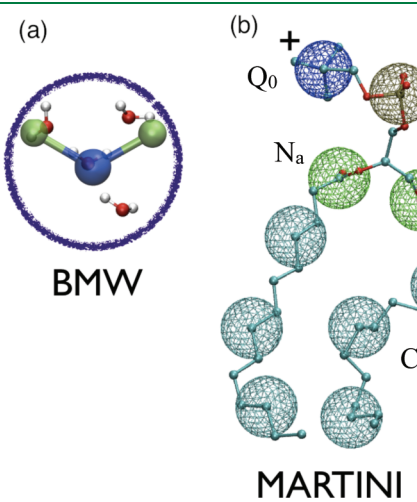


Figure 1. Mapping between the chemical structure and the CG model for water and DMPC lipid. Topologies for nonwater components are taken directly from MARTINI.

Several modifications are made to the CG particle (or bead) types in MARTINI. First, water specific types are added. The modified BMH potential is used for BMW-BMW (only between the charge-negative sites), while LJ is used for all other interactions, including those between BMW and other bead types. The antifreezing particle type BP4 is deleted, because with the soft interaction the BMW water does not (unphysically) freeze, and antifreeze particles are therefore not required. Second, a super repulsive (with $\sigma = 0.62$ nm) interaction between charged (Q) and apolar (C) types is no longer needed, because the interaction between charged beads is now characterized by Coulombic interactions with a small amount of screening (the screening dielectric constant in the BMW model is 1.3 instead of 15–20 in the original MARTINI). Subtypes AC1 and AC2 are therefore deleted in the new force field, and all Q–C interactions are assigned with $\sigma = 0.47$ nm ($\sigma = 0.43$ nm between bead types in rings). Finally, new subtypes are added for amino acids to introduce additional flexibility: RQ_d for guanidinium group in arginine and AQ_a for aspartate and glutamate. For ions and peptide terminal groups, the Q_d subgroups are the same, while all Q_a subgroups are replaced by AQ_a (e.g., for Cl⁻).

For the nonelectrostatic interaction levels among bead types, those between groups of P, N, and C are mostly inherited from MARTINI, except for the following: P₅ and P₄ interact with N_{da}, N_d, and N_d with $\varepsilon = 5.6$ kJ/mol; all ring beads (label starting with S) interact with C1 with a scaling factor of 90% for the original ε in MARTINI. By contrast, bead–water interactions have to be modified to reproduce relevant hydration and transfer free energies. Similar to the polarizable MARTINI model,³⁶ scaling factors for the well-depths, ε , are introduced to reduce the strength of interaction (relative to the original MARTINI) between uncharged bead types and water (BMW); the factor is 71% for levels with $\varepsilon < 4.5$ kJ/mol in the original MARTINI and 75% otherwise. Furthermore, nonelectrostatic interactions between charged groups (type Q) and all other beads are modified, since electrostatic interactions are treated differently in the new model. As shown in Table 1, besides Q–Q and Q–BMW interactions, levels for Q to other uncharged groups, especially apolar types (C), are also tuned to ensure reasonable partitioning free energies. This is required because hydration free energies of charged groups are altered upon using the BMW model for water. Meanwhile, levels for Q–P and P–N interactions remain very similar to the original MARTINI because the nonpolar interactions between these bead types still implicitly represent both van der Waals and dipolar/hydrogen-bonding contributions.

The bonded parameters (e.g., bond, angle, and torsional angle force constants) for the new CG model are largely the same as the

Table 1. Levels of Nonpolar Interactions among Charged Groups, BMW Water, and Uncharged Groups in the BMW-MARTINI Model^a

BMW	Q						P				N				C					
	Q _{da}	Q _d	RQ _d	Q _a	Q _{da}	Q _o	P ₅	P ₄	P ₃	P ₂	P ₁	N _{da}	N _d	N _a	N _o	C ₅	C ₄	C ₃	C ₂	C ₁
Q _{da}	I	O	O	O	O	O	II	O	O	O	I	I	O	O	O	IV	III	IV	IV	IV
Q _d	I	O	I	I	O	O	II	O	O	O	I	I	O	III	O	IV	III	IV	IV	IV
RQ _d	IV	O	I	I	O	O	II	O	O	O	I	I	O	III	O	IV	III	IV	IV	IV
Q _a	I	O	O	O	I	I	II	O	O	O	I	I	O	O	III	IV	III	IV	IV	IV
AQ _a	I	O	O	O	I	I	II	O	O	O	I	I	O	O	III	IV	III	I	I	I
Q _o	I	II	II	II	II	IV	I	O	I	II	III	III	III	III	IV	III	IV	IV	IV	IV

^a Level of interaction indicates the well depth in the LJ potential: O, $\varepsilon = 5.6$ kJ/mol; I, $\varepsilon = 5.0$ kJ/mol; II, $\varepsilon = 4.5$ kJ/mol; III, $\varepsilon = 4.0$ kJ/mol; IV, $\varepsilon = 3.5$ kJ/mol; V, $\varepsilon = 3.1$ kJ/mol; VI, $\varepsilon = 2.7$ kJ/mol; VII, $\varepsilon = 2.3$ kJ/mol; and VIII, $\varepsilon = 2.0$ kJ/mol. The LJ parameter $\sigma = 0.47$ nm ($\sigma = 0.43$ nm for rings) is used for all interaction levels. The same grouping criteria (including subgroups) are applied as in the original MARTINI scheme.¹⁵

original MARTINI. Only the force constant for angle bending in hydrocarbons (lipid tails) is modified from 25 to 10 kJ/(mol·degree²), because it is reported that the angle distribution in MARTINI is narrower than the atomistic counterpart.⁴⁹ Also, the scheme of restraining secondary structure elements in MARTINI is adopted, and relieving such restraints⁵⁰ will be an interesting direction for further developments.

D. Simulation Protocols. The simulation protocols used for the new CG model are largely the same as for BMW water simulations.⁴¹ A time step of 20 fs is used with GROMACS 4.0.5.⁵¹ Temperature and pressure are kept constant by using the Berendsen scheme,⁵² with coupling times of $\tau_T = 1$ ps and $\tau_P = 5$ ps. The SETTLE algorithm⁵³ is used to constrain “bonds” in CG water, and LINCS⁵⁴ is used for bonds in ring structures in several amino acids. PME with a spacing of 0.2 nm and $\epsilon_r = 1.3$ are applied for electrostatics. Similar to the original MARTINI, LJ interactions are excluded between bonded beads but not for second nearest neighbors. The shift cutoff scheme ($r_{\text{shift}} = 0.9$ nm and $r_{\text{cut}} = 1.2$ nm) is applied to all LJ interactions, while the switch scheme ($r_{\text{switch}} = 1.2$ nm and $r_{\text{cut}} = 1.4$ nm) is used for water–water BMH interactions (see Supporting Information for details). With these protocols, simulations with the new force field are slower than the original MARTINI but about 2–3 orders of magnitude faster than atomistic simulations. As discussed in MARTINI applications,¹⁵ since the lipid lateral diffusion rate is about 4 times larger than experimental measurement, time scales in all simulation are interpreted as 4 times the actual simulation lengths.

E. Properties Calculated. The free energies of hydration and partitioning between water and octanol for a number of n-alkanes are calculated using thermodynamic integration (TI),^{55,56} which is carried out at 300 K with 21 evenly spaced λ windows, where λ is the coupling parameter in the TI method, each sampled for 160 ns; the target bead is decoupled from its surrounding solvents with a soft core potential.

The area per lipid of lipid bilayers is calculated from $NP_{xy}P_z T$ simulations, where N is the number of molecules, P_{xy} and P_z are the transverse and normal components of the pressure tensor, and T is the temperature. Patches of 512 lipids are simulated with a hydration level of ~60 water molecules per lipid; the results are averaged over 240 ns production run after equilibration.

The area compressibility modulus, K_A , is calculated from the relation between membrane area per lipid A, tension-free equilibrium area per lipid A_0 and surface tension γ (eq 1):⁵⁷

$$K_A = 2A_0 \left(\frac{\partial \gamma}{\partial A} \right)_T \quad (1)$$

$NA_{xy}P_z T$ simulations are performed on dipalmitoylphosphatidylcholine (DPPC) lipids with five different restrained membrane areas (evenly from 60 to 68 Å²/lipid in the xy plane), and the corresponding surface tension per leaflet γ is calculated. Test calculations indicate only a small finite size effect on the calculated K_A , with the difference between a bilayer patch of 128 and 512 lipids being within statistical uncertainties.

The line tension is computed by constructing a ribbon structure of bilayers, continued in the z direction as shown in Figure 2. This structure is simulated in the $NP_{xy}L_z T$ (325 K) ensemble, and line tension is calculated from the edge along z from eq 2:⁵⁸

$$\Lambda = \frac{1}{2} \left\langle L_x L_y \left[\frac{P_{xx} + P_{yy}}{2} - P_{zz} \right] \right\rangle \quad (2)$$

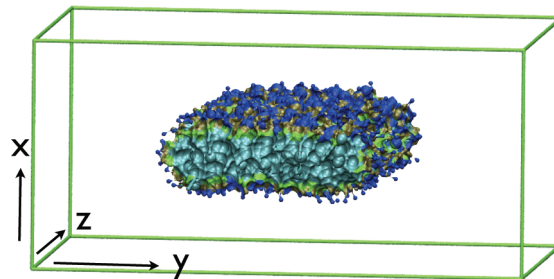


Figure 2. Ribbon structure of 512 DPPC lipids and the simulation box (shown with VMD)⁵⁹ in the line tension calculation. For clarity, all waters (16 096 BMW water) are omitted, and the ribbon is intersected in the x – y plane as shown, with tails in cyan, glycerol in green, and head groups in tan and blue.

III. RESULTS AND DISCUSSION

A. Free Energies of Hydration and Partitioning. Calibration of free energies of hydration and partitioning between water and hexadecane plays an important role in the development of GROMOS and MARTINI force fields. We also use these quantities to calibrate LJ interaction parameters for uncharged bead types in the BMW-MARTINI model. For charged groups, due to the lack of relevant experimental data, they are parametrized based on lipid properties and amino acid PMFs, as described in later sections.

Due to the CG nature of the model, it is only meaningful to compare calculated free energies with experimental values for a range of similar compounds, as was done with the original MARTINI model. As shown from Table 2, results with the new CG model are overall in good agreement with experimental and original MARTINI results. Thus simply using two scaling factors for the LJ well-depth between uncharged groups and water is sufficient for the current purpose. Due to the soft-core nature of the BMW model, which allows smaller energy variation upon solute insertion, the scaling factors are smaller than the one (95%) introduced in the polarizable MARTINI model.³⁶ Similar to the original MARTINI model,¹⁵ our model systematically underestimates the hydration free energies as compared to experimental values. The magnitude of the underestimation is larger for more polar beads (i.e., P groups), indicating that improving the description of polar groups (e.g., by including explicit dipoles) can be a future direction for development. Since our current model mainly focuses on the partitioning of beads between polar and apolar environments, as in the original MARTINI, interactions between P and C groups are underestimated to compensate for the underestimated hydration of P groups. For charged particles, because electrostatics are explicitly included in the new model, the solvation free energies are comparable to atomistic results (also see Supporting Information for discussions of ions).

B. Hydration Thermodynamics. In addition to comparing hydration free energies, it is of interest to compare the enthalpic–entropic components of hydration at the CG and atomistic levels to ensure that the CG model captures the proper physics of solvation, especially that of hydrophobic groups. For this purpose, we study the hydration of N-hexadecane (four bonded C1 beads in the CG model), which forms the tail of DPPC. Solvation free energies computed at different temperatures (263–343 K) are decomposed into solute–solvent interaction energy U_{uv} and

Table 2. Free Energy of Hydration and Partition between Water and Hexadecane for Neutral Groups Is Compared to Experimental Values for Target Compounds and MARTINI^a

scaling factor	type	hydration			partition		
		expt.	MARTINI	BMW	expt.	MARTINI	BMW
75%	P ₅	-40	-25	-21	-27	-28	-27
	P ₄	-27~−35	-18	-15	-21~−25	-23	-22
	P ₃	-29	-18	-15	-19	-21	-19
	P ₂	-21	-14	-11	-13	-17	-14
	P ₁	-20~−21	-14	-11	-9~−10	-11	-10
71%	N _d /N _a /N _{da}	-12~−20	-9	-5	-4~−6	-7	-4
	N ₀	-8	-2	-1	-1	-2	0
	C ₅	-6	1	2	7	5	7
	C ₄	-4~−2	5	5	7~11	9	10
	C ₃	-1~−2	5	5	12	13	14
	C ₂	8	10	8		16	17
	C ₁	9~10	14	10	18	18	19

^aThe estimated experimental values are taken directly from ref 15 and compound names are not listed here. The scale in the first column is the scaling factor for MARTINI potential levels between the groups and water. All units are in kJ/mol, and the new model is labeled as BMW.

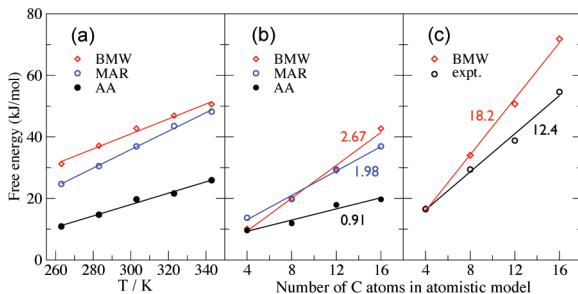


Figure 3. Hydration free energy in water for (a) n-hexadecane as a function of temperature and (b) n-alkanes at 303 K. Panel (c) shows the partition free energy for n-alkanes between water and octanol at 303 K. Data for both atomistic (AA) and MARTINI (MAR)¹⁴ are taken directly from ref 61, while the partitioning data are compared to experimental values (expt.).⁶² The corresponding linear regression curves and their slopes are also displayed in the same color.

entropy S_{uv} ,⁶⁰ and the results are compared to both atomistic and MARTINI results.⁶¹

In all cases, the hydration free energies predicted by our new CG model are similar to the original MARTINI model, and systematically overestimate the atomistic value for the free energy at all temperatures, as can be seen in Figure 3. Decomposition of the solvation free energy into enthalpic and entropic terms (not shown) indicates that both models overestimate both the solute–solvent interaction energy and the entropy by significant amounts (of the order of 50 kJ/mol and 100–200 kJ/(mol·K), respectively), i.e., this does not simply originate from an overestimation of the water–oil repulsion as previously reported.⁶¹ As the chain length increases (Figure 3b), the enthalpic contribution in the CG models decreases more slowly compared to atomistic results, while contributions from entropy ($−TS$) change at a similar pace in the three models. In other words, with a CG model, change in the solute–solvent enthalpy as the chain elongates is not strong enough to compensate for the change in solute–solvent entropy.

For the partition free energy of solutes between water and octanol (see Figure 3c), the discrepancy between CG and atomistic

Table 3. Area Per Lipid for Common Saturated and Unsaturated PC, PE, and PS Phospholipids in the CG Model^a

systems	expt.	MARTINI	BMW
DPPC (325 K)	63 ⁶³	64	64
DPPC (338 K)	64–67 ^{65,66}	66	65
DOPC (300 K)	67 ⁶⁴	67	64
DOPE (273 K)	65 ⁶⁷	61	60
DOPS (303 K)	65 ⁶⁸	67	62

^aAll units are in Å². Typical uncertainties in simulation results and experiments are 1 and 2 Å², respectively. For MARTINI, all values are shown as reported in ref¹⁴ except for DOPS, which is calculated from this work.

results is less sensitive to the chain length, due likely to error cancellation. This is encouraging because partition free energies are more important for the development of both original and our improved MARTINI model.

C. Lipid Properties. *1. Bilayer Structural, Elastic, and Dynamic Properties.* The BMW-MARTINI model values for the area per lipid in bilayers are similar (somewhat lower) to that obtained from experiment or from the MARTINI model. Table 3 compares the area per lipid obtained from various models for several common saturated, unsaturated, and charged lipid bilayers. Given the uncertainty in experimental measurements, the results from the new model are satisfying, especially for charged lipids, such as DOPS. Similar agreement is found for the thickness of lipid bilayers. For DPPC bilayers (at 325 K), the experimentally measured thickness is 3.8 nm,⁶³ MARTINI gives 4.0 nm, and BMW-MARTINI gives 3.9 nm. For DOPC bilayers (at 300 K), both the original MARTINI (4.5 nm) and BMW-MARTINI (4.6 nm) values are larger than the experimental result (3.7 nm).⁶⁴ Considering the CG nature of the lipid tails (one bead representing ~4 CH₂ groups), the agreement can be considered satisfactory. Furthermore, the density profiles of the CG bilayer are in good agreement with experiment (see Supporting Information).

The BMW-MARTINI results for the area compressibility modulus, K_A , and the line tension are significantly higher than the experimental values or those obtained from the MARTINI

model. For DPPC bilayers, the BMW-MARTINI prediction for K_A is 585 ± 16 dyn/cm, which is higher than the experimental value⁶⁹ of 234 dyn/cm and the MARTINI result of 292 dyn/cm (also calculated using eq 1). The model predicts a line tension of 118 ± 11 pN, which is higher than the experimental estimate of $10\text{--}30$ pN for similar lipids^{70–72} and the MARTINI value of 64 pN.⁷³

The high line tension in the BMW-MARTINI model will likely result in the model significantly overestimating the barrier to pore formation in lipid bilayers. The energy E required to form a pore inside the bilayers can be approximated by⁷⁴ $E(r) = 2\pi\Lambda - \pi r^2\gamma$, where r is the pore radius and γ the tension on membrane. At the critical tension γ^* , the edge energy from Λ is overcome, and a pore is stable at $r = \gamma^*/\Lambda$. Therefore, overestimating Λ means that the critical tension required to form a pore is likely to be overestimated. The overestimated line tension is likely related to the CG nature of the solvent, where the partitioning of individual water molecules at the bilayer edge is not captured. By grouping four waters together into a single site, the energy penalty for bringing a CG water into the hydrophobic region becomes larger. This energy penalty is large in the BMW-MARTINI model, compared to the MARTINI model, because of the presence of electrostatic interactions.

The lipid (DPPC) lateral diffusion constant is $0.8 \pm 0.1 \times 10^{-7}$ cm²/s (using the effective scaling factor of 4 due to coarse-graining),¹⁵ which is similar to the experimental value of 1.0×10^{-7} cm²/s.⁷⁵

2. Lipids Self-Assembly. The microphase morphology of lipids is an important benchmark for interaction parameters of charged groups. Experimental studies indicate that DOPE lipids assemble into an inverted hexagonal phase at temperatures above 280–300 K with 1:16 lipid/water hydration level,⁷⁶ while DOPC lipids assemble into the lamellar phase under similar conditions.⁷⁷ This phase behavior reflects the spontaneous curvature of the lipid layers, which are negative for DOPE and about zero for DOPC.^{78,79} The interactions between lipid head groups (Q–Q) and between the head groups and water (Q–BMW) play a key role, since they modulate the effective shape of the lipid molecules (e.g., cone vs cylinder).

The BMW-MARTINI model gives the correct phases for DOPE and DOPC, which suggests that the spontaneous curvatures for bilayers of both lipids are properly captured by the current model. To study the phase behavior of lipids, a system of 1000 lipids mixed randomly with 4000 CG solvents (corresponding to 16 water molecules per lipid) is simulated with completely anisotropic pressure coupling at 318 K. Because the lamellar phase has a faster water exchange rate, it is prepared as the initial configuration: A lamellar phase is first assembled by artificially setting the lipid head groups to interact with water with the highest interaction strength in the MARTINI force field (level O), then the proper level of interaction is used for subsequent simulations. For DOPE, “stalks” of lipids are gradually formed between the lamellar layers, and the inverted hexagonal phase is formed within $\sim 5 \mu\text{s}$ (shown in Figure 4). The resulting hexagonal spacing (distance between the central axes of water channels) is 6.8 nm, which agrees well with the estimate from SAXS data as 7.1 nm.⁸⁰ For DOPC, no stalk formation is observed, and the lamellar phase remains stable for the subsequent 5 μs simulations, and the resulting lamellar repeat spacing is 5.8 nm; the experimental value for fully hydrated lipids is 6.3 nm.⁶³

3. Membrane Interface Electrostatic Properties. The dipole potential at the membrane-water interface is significantly improved

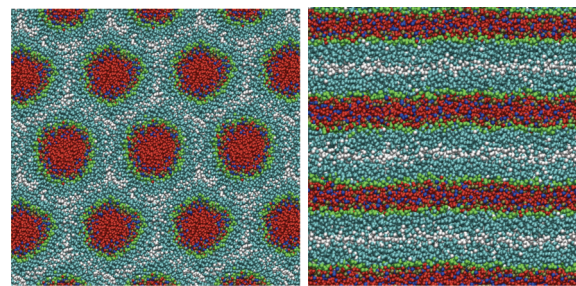


Figure 4. BMW-MARTINI results for the inverted hexagonal phase of DOPE (left) and lamellar phase of DOPC (right); the beads are color coded: water in red, lipid tails in cyan, glycerol in green, lipid head groups in blue and tan, and lipid tail terminals (last bead) in white.

with the BMW model over previous CG models, such as MARTINI.⁴¹ With refined parameters in this work, this feature is maintained. The calculated value of the interfacial potential is +0.23 V (the value was +0.30 V with a preliminary combination⁴¹ of BMW and MARTINI lipid models), in good agreement with experimental estimates of 0.22–0.28 V for DPPC bilayers.³⁰

D. Interaction between Amino Acids and a Lipid Bilayer. *1. Partition of Amino Acid Side Chains.* The PMF is calculated for each amino acid side chain as a function of the distance from the center of a DOPC lipid bilayer. Results are compared to both atomistic⁴⁸ and MARTINI²³ models to further fine-tune interaction levels in our CG model, especially for charged groups. For each simulation, two side chain analogues are placed at a distance of 4.5 nm from each other, one in the center of bilayer and the other in the bulk, in a system of 96 DOPC lipids and 1300 BMW waters; the PMF is then calculated with the standard umbrella sampling protocol, with 46 windows and 80 ns for each window, and force constants of ~ 1000 kJ/(mol·nm²). The PMF is averaged over the symmetric halves of the bilayer. For charged side chains, two ions (Na⁺ or Cl⁻) are added to maintain charge neutrality.

Some of the parameters are fine-tuned after a comparison with atomistic results, so this is strictly not a test of the model. New bead types are introduced: RQ_d for the arginine guanidinium group and AQ_a for aspartate and glutamate. The other side chains are represented with the same topology as MARTINI. For neutral amino acids the parameters are not changed beyond what was used for the partition free energy between water and hexadecane (Table 2). For the aromatic side chains, a scaling factor of 90% for all the ring groups (start with S) to C1 is applied. New parameters are fit for the charged side groups. For highly polar but neutral side chains, Gln (P₄) and Asn (P₅), their interactions to N_{da}, N_d, and N_a are changed as $\epsilon = 5.6$ kJ/mol.

The new force field is more accurate for the side chain PMF than the MARTINI force field, when compared to results from atomistic simulations. In Figure 5, representative PMF profiles for hydrophobic, polar, aromatic, and charged amino acid side chain analogues are shown. For neutral amino acids, the PMFs have the proper values in both solution and membrane tail regions. PMF in the interfacial region is determined by interactions between charged groups (lipid head groups) and the side chain. Take leucine for example, modeled as C₁, the scaling factor for the nonpolar interactions determines its insertion PMF between water and the bilayer center, and the barrier at the interface is defined by Q–C₁ interactions. Both the original MARTINI and the BMW-MARTINI are accurate for these PMFs. For the polar amino acids the performance of the new force field is slightly superior to the MARTINI force field, but

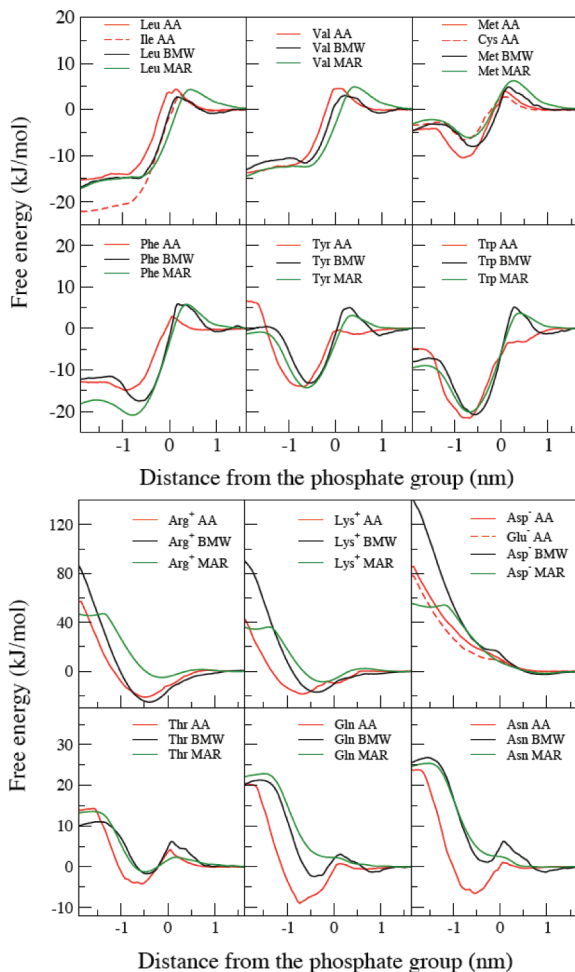


Figure 5. Insertion PMF for amino acids into a DOPC bilayer (negative distances indicate the interior of the bilayer). Note that although the position of phosphate groups is strictly defined with electron density maximum for each model, the position of the amino acid relative to the phosphate (*x*-axis) in the MARTINI and BMW-MARTINI models is subject to some uncertainty (up to 0.2 nm) due to the CG nature of these models. Both atomistic (AA)⁴⁸ and MARTINI (MAR)²³ data are obtained from Tielemans and co-workers (private communication).

neither force field is in quantitative agreement with the atomistic simulation results.

For the charged amino acids, their PMFs are closely coupled to membrane–water defects induced by the penetration of the side chains. This makes the parametrization more complicated than for neutral groups because all Q–Q, Q–BMW, Q–neutral interactions should, in principle, be considered. However, since our model gives the correct electrostatic profile at the interface, a deep minimum is always observed for the cationic side chains although the depth of the minimum depends on the parametrization. Compared with the original MARTINI (Arg^+ : -6 kJ/mol and Lys^+ : -9 kJ/mol), our new model gives a substantially deeper minimum: -22 kJ/mol for arginine and -20 kJ/mol for lysine; the latter values are close to the atomistic results. In the center of the bilayer, the calculated PMF with BMW-MARTINI is too high for all charged amino acids compared to atomistic results. However, even different atomistic force fields give rather different values in this region with an uncertainty up to 25 kJ/mol .⁸¹ Therefore, we do not consider the discrepancy in this region as a

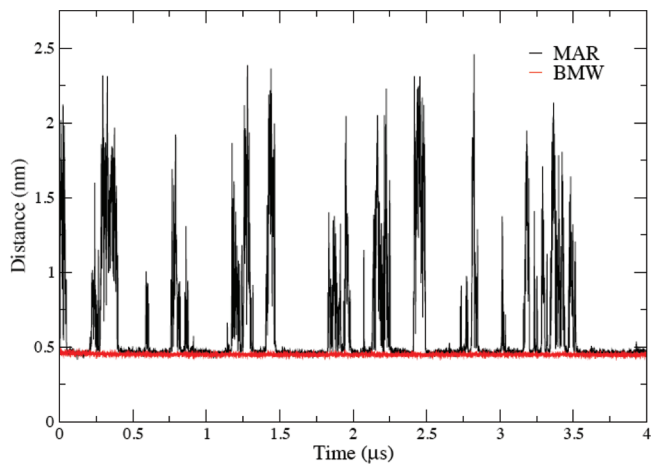


Figure 6. The minimum distance between Poly-Arg₈ and a DOPC bilayer as a function of time from MARTINI (MAR) and BMW-MARTINI (BMW) simulations. The van der Waals diameter of the relevant bead types is 0.47 nm, thus the peptide is considered attached to the surface if the minimum distance is below 0.47 nm. Somewhat similar differences are observed also for Poly-Arg₈ at the surface of an anionic membrane (70% DOPC and 30% DOPS).

significant limitation of the model, although this issue deserves further exploration especially in the context of studying pore formation, where the line tension of the bilayers will play an important part.

2. Poly-Arg₈ Attachment on Membrane. We use the new force field to investigate the attachment of peptides to a membrane surface. Simulations of a poly-Arg₈ cationic peptide (analogue to HIV-TAT peptide)⁸² on the surface of a 128 DOPC lipid bilayer are performed with both the new model and original MARTINI; the simulation cells are charge neutral with counterions (0.15 M NaCl) (see details for ion in Supporting Information). According to recent experimental observations,⁸³ the peptide attaches to the membrane surface with a long residence time of up to a second; atomistic simulations^{82,84} up to 400 ns also showed stable attachment. With the original MARTINI, the peptide does not absorb in a stable fashion and desorbs frequently with the longest residence time on the membrane surface of ~ 350 ns (Figure 6a).

The BMW-MARTINI model predicts a stable attachment of poly-Arg₈ to a DOPC bilayer. Figure 6 depicts the minimum distance between the peptide and the bilayer as a function of time and shows that with the BMW-MARTINI model the peptide stays attached up to tens of microseconds (throughout the entire simulation) unlike the original MARTINI model. On the surface of an anionic bilayer (70% DOPC and 30% DOPS), the new model gives very stable attachment of poly-Arg₈. With MARTINI, however, the peptides are still observed to desorb from the membrane surface although the residence time ($\sim \mu\text{s}$) is longer than that at the surface of a zwitterionic (DOPC) bilayer. This difference is anticipated based on the difference in the insertion PMF for arginine side chains at the membrane surface (see Figure 5 on DOPC), for which the MARTINI model predicts a much shallower minimum than the BMW-MARTINI model. This qualitative difference between BMW-MARTINI and MARTINI highlights the importance of properly describing electrostatics for the analysis of highly charged peptides or protein motifs near membrane surface.

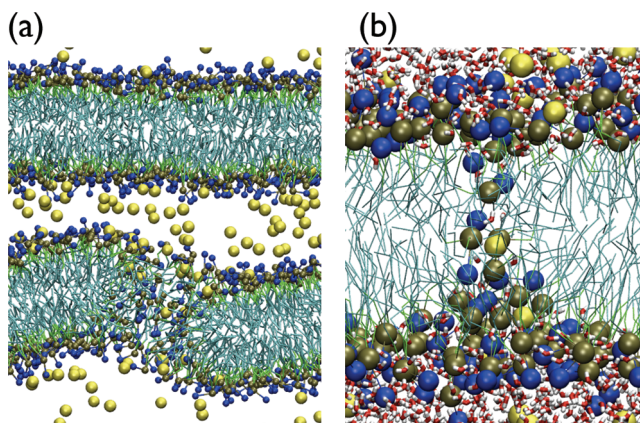


Figure 7. Snapshots from simulations of electroporation (with an initial charge imbalance of 26 e^-). (a) The initial structure of the pore, formed within 1 ns (the water molecules are omitted for clarity). (b) The final structure of the (toroidal) water defect. Color code: yellow: Na^+ or Cl^- ; blue: choline; and tan: phosphate.

In a recent study³⁷ of insertion PMF for pentapeptides that feature both charged and hydrophobic groups, Singh and Tieleman found that the polarizable MARTINI model leads to a substantial improvement over the original MARTINI, and the results were in good agreement with atomistic simulations. This is interesting because the interfacial potential calculated by polarizable MARTINI still has the incorrect sign.³⁶ On the other hand, as analyzed by Allen and co-workers,³⁸ the membrane permeation energetics for charged groups are not a simple function of the interfacial potential because the dipole potential is not fully sensed at the locally deformed bilayer interface. Moreover, the presence of both hydrophobic and charged groups in the pentapeptides may have further helped attenuate the errors associated with the charged group. In the near future, as the amino acids parameters for the polarizable MARTINI model³⁶ become available, it is valuable to compare the BMW-MARTINI and polarizable MARTINI models in a systematic fashion.

Simulations with multiple copies of poly-Arg₈ (in the presence of Na^+/Cl^- counterions) on a DOPC bilayer show no membrane penetration during up to $20\text{ }\mu\text{s}$, in agreement with more recent atomistic simulations.⁸⁴ With 8 peptides, the area per lipid increases slightly from the peptide-free value of $0.64\text{--}0.66\text{ nm}^2$. Order parameter calculations indicate that the head groups become more ordered and perpendicular to the membrane normal in the presence of multiple cationic peptides; at the same time, water clusters near the membrane surface (below phosphate groups) become slightly less ordered.

Finally, interesting phase behaviors have been observed experimentally for the mixture of cationic peptides (e.g., poly-Arg vs poly-Lys) and lipids.⁸⁵ Simulations with a reliable CG model are expected to be very effective at complementing experiments to better understand the connections between peptide sequence and phase behavior.⁸⁶ Such studies are in progress and will be reported separately.

3. Electroporation. When two bilayers are constructed with an imbalance of ions on the two sides, the chemical potential difference and local electric field drive the transfer of ions through the bilayer via the formation of a water pore. The process is referred to as electroporation and has been used to test both atomistic^{87,88} and CG³⁶ lipid models. Here we investigate the same systems studied previously by the polarizable MARTINI model.³⁶ A typical

system consists of two DPPC bilayers, which contain 512 lipid molecules, 5632 CG BMW water molecules, 52 evenly distributed (over the two water compartments) Cl^- ions and 52 Na^+ in one water compartment; this charge imbalance of 26 e^- results in an electric field of 0.7 V/nm . Simulations are performed in the $NP_{xy}P_zT$ ensemble, at 325 K , and for $6\text{ }\mu\text{s}$.

With this charge imbalance, the simulations show the opening of a water pore, transportation of both Na^+ and Cl^- ions, and then closing of the pore. Typically, a water pore is formed within 1 ns, and ions diffuse from one water compartment to the other through the pore (shown in Figure 7a); Na^+ and Cl^- ions translocate in opposite directions during the process. The water pore grows in size until approximately $20\text{--}40\text{ ns}$, when it reaches its maximum diameter ($\sim 4\text{ nm}$) and then starts to shrink in size. After approximately 100 ns , only a water defect remains with about 5 CG water in the membrane interior. With the small charge imbalances at this stage, the ions still translocate through a toroidal pore (shown in Figure 7b), in agreement with previous atomistic simulations.⁸⁸ By contrast, the defect observed at this stage with the polarizable MARTINI model does not involve significantly displaced lipid headgroups and thus closer to the barrel stave model.³⁶ Eventually, after approximately 400 ns , the water defect completely seals, and the two compartments have different concentrations of ions (containing about $36\text{ Na}^+/34\text{ Cl}^-$ and $16\text{ Na}^+/18\text{ Cl}^-$, respectively) with a negligible charge imbalance of $1\text{--}2\text{ e}^-$.

Spontaneous electroporation also occurs for smaller (20 e^-) and larger (52 e^-) charge imbalances. For large charge imbalances, multiple pores located on different bilayers are observed. With a smaller charge imbalance (20 e^-), pore formation takes a longer time, which could be several μs . The total number of Na^+ and Cl^- transferred to the opposite water compartment is similar if the initial charge imbalance is small, indicating little membrane selectivity toward anions (Cl^-) over cations (Na^+), in agreement with atomistic studies.⁸⁸

IV. CONCLUSIONS

We report a new CG force field, called BMW-MARTINI, for simulations of lipids and peptides in water. The model follows the same strategy as the original MARTINI force field but is based on the BMW water model, which includes electrostatic interactions. The interactions between almost all the CG sites are reparameterized.

The new force field provides a reasonably accurate description of the hydration of the CG sites, the transfer free energy of sites between hexadecane and water, lipid phase behavior, membrane electrostatic properties, and insertion potential of mean force for amino acids into a bilayer. For most of these properties, the BMW-MARTINI model gives similar results as the original MARTINI.

For membrane electrostatic properties and the insertion potential of mean force of charged amino acids into a bilayer, the new model is superior to both the original and the polarizable MARTINI models and predicts a much deeper free energy minimum at the membrane–water interface. As a consequence, the new model predicts a stable attachment of cationic peptides to both zwitterionic and negatively charged membrane surfaces, as observed in experiment and atomistic simulation, while frequent desorptions are observed with the original MARTINI force field. The model also predicts electroporation when there is a charge imbalance across the lipid bilayer, in contrast to the original MARTINI. The pore formed during electroporation is

toroidal in nature, similar to the prediction of atomistic simulations but distinct from results of polarizable MARTINI for small charge imbalances.

In terms of efficiency, the new model is more computationally intensive than the nonelectrostatic MARTINI by a factor of less than 6, but still more than 2 orders of magnitude more efficient than atomistic models. Therefore, the BMW-MARTINI model is a useful alternative to the (polarizable) MARTINI model, and future studies are required to systematically compare the merits and limitations of these models in realistic applications.

In the current form, the BMW-MARTINI model is not as accurate for the mechanical properties of the membrane, with values for the area compressibility modulus and line tension being significantly higher than experiment or the original MARTINI model. We attribute this to the mapping of four water molecules to one CG site which makes the process of transferring a water from the aqueous phase to hydrophobic region unrealistic. The electrostatic interactions in the BMW water model exacerbate this problem with the coarse-graining procedure. This overestimation of mechanical properties is likely to result in a high barrier to pore formation. A possible solution to this problem is to use an adaptive resolution scheme for water,^{89,90} where CG sites can be transformed into atomistic water molecules in the interface and pore region. Alternatively, soft interactions, which are limited to water–water interactions in the current model, can be introduced between water and other components of the system.

■ ASSOCIATED CONTENT

Supporting Information. Additional benchmark results and discussions are included. This material is available free of charge via the Internet at <http://pubs.acs.org>.

■ AUTHOR INFORMATION

Corresponding Author

*E-mail: cui@chem.wisc.edu; yethiraj@chem.wisc.edu.

■ ACKNOWLEDGMENT

We thank Prof. P. Tieleman and Dr. L. Monticelli for sharing the insertion PMF data for amino acids into a lipid bilayer, for sending us the preprint of ref 37, and for a critical reading of the manuscript. The research has been supported by the National Science Foundation (CHE-0957285 to QC and CHE-0717569 and CHE-1111835 to A.Y.). Computational resources from the National Center for Supercomputing Applications at the University of Illinois and the Centre for High Throughput Computing (CHTC) at UW-Madison are greatly appreciated. Computations are also supported in part by National Science Foundation through a major instrumentation grant (CHE-0840494).

■ REFERENCES

- (1) Phillips, R.; Ursell, T.; Wiggins, P.; Sens, P. *Nature* **2009**, *459*, 379–385.
- (2) Andersen, O. S.; Koeppke, R. E., II. *Annu. Rev. Biophys. Biomol. Struct.* **2007**, *36*, 107–130.
- (3) Huang, H. W. *Biochem.* **2000**, *39*, 8347–8352.
- (4) Chapman, E. R. *Annu. Rev. Biochem.* **2008**, *77*, 615–641.
- (5) Doherty, G. J.; McMahon, H. T. *Annu. Rev. Biochem.* **2008**, *77*, 65–95.
- (6) Tang, Y.; Cao, G.; Chen, X.; Yoo, J.; Yethiraj, A.; Cui, Q. *Biophys. J.* **2006**, *91*, 1248–1263.
- (7) Chen, X.; Cui, Q.; Tang, Y. Y.; Yoo, J.; Yethiraj, A. *Biophys. J.* **2008**, *95*, 563–580.
- (8) Ma, L.; Yethiraj, A.; Chen, X.; Cui, Q. *Biophys. J.* **2009**, *96*, 3543–3554.
- (9) Tozzini, V. *Curr. Opin. Struct. Biol.* **2005**, *15*, 144–150.
- (10) Clementi, C. *Curr. Opin. Struct. Biol.* **2008**, *18*, 10–15.
- (11) Ayton, G. S.; Noid, W. G.; Voth, G. A. *Curr. Opin. Struct. Biol.* **2007**, *17*, 192–198.
- (12) Marrink, S. J.; de Vries, A. H.; Tieleman, D. P. *Biochim. Biophys. Acta, Biomembr.* **2009**, *1788*, 149–168.
- (13) Shinoda, W.; DeVane, R.; Klein, M. L. *J. Phys. Chem. B* **2010**, *114*, 6836–6849.
- (14) Marrink, S. J.; de Vries, A. H.; Mark, A. E. *J. Phys. Chem. B* **2004**, *108*, 750–760.
- (15) Marrink, S. J.; Risselada, H. J.; Yefimov, S.; Tieleman, D. P.; de Vries, A. H. *J. Phys. Chem. B* **2007**, *111*, 7812–7824.
- (16) Marrink, S. J.; Mark, A. E. *J. Am. Chem. Soc.* **2003**, *125*, 15233–15242.
- (17) Marrink, S. J.; Mark, A. E. *J. Am. Chem. Soc.* **2003**, *125*, 11144–11145.
- (18) Kasson, P. M.; Kelley, N. W.; Singhal, N.; Vrljic, M.; Brunger, A. T.; Pande, V. S. *Proc. Natl. Acad. Sci. U.S.A.* **2006**, *103*, 11916–11921.
- (19) Smirnova, Y. G.; Marrink, S. J.; Lipowsky, R.; Knecht, V. *J. Am. Chem. Soc.* **2010**, *132*, 6710–6718.
- (20) Marrink, S. J.; Mark, A. E. *Biophys. J.* **2004**, *87*, 6710–6718.
- (21) Baoukina, S.; Monticelli, L.; Risselada, H. J.; Marrink, S. J.; Tieleman, D. P. *Proc. Natl. Acad. Sci. U.S.A.* **2008**, *105*, 10803–10808.
- (22) Risselada, H. J.; Marrink, S. J. *Proc. Natl. Acad. Sci. U.S.A.* **2008**, *105*, 17367–17372.
- (23) Monticelli, L.; Kandasamy, S. K.; Periole, X.; Larson, R. G.; Tieleman, D. P.; Marrink, S. J. *J. Chem. Theory Comput.* **2008**, *4*, 819.
- (24) Yefimov, S.; van der Giessen, E.; Onck, P. R.; Marrink, S. J. *Biophys. J.* **2008**, *94*, 2994–3002.
- (25) Yoo, J.; Cui, Q. *Biophys. J.* **2009**, *97*, 2267–2276.
- (26) Lu, L. Y.; Voth, G. A. *J. Phys. Chem. B* **2009**, *113*, 1501–1510.
- (27) Deserno, M. *Macromol. Rapid Commun.* **2009**, *30*, 752–771.
- (28) Wang, Z. J.; Deserno, M. *J. Phys. Chem. B* **2010**, *114*, 11207–11220.
- (29) Lin, J. H.; Baker, N. A.; McCammon, J. A. *Biophys. J.* **2002**, *83*, 1374–1379.
- (30) Clarke, R. J. *Adv. Colloid Interface Sci.* **2001**, *89*, 263–281.
- (31) Shapovalov, V. L.; Kotova, E. A.; Rokitskaya, T. I.; Antonenko, Y. N. *Biophys. J.* **1999**, *77*, 299–305.
- (32) Siu, S. W. I.; Vácha, R.; Jungwirth, P.; Böckmann, R. A. *J. Chem. Phys.* **2008**, *128*, 125103.
- (33) Harder, E.; MacKerell, A. D.; Roux, B. *J. Am. Chem. Soc.* **2009**, *131*, 2760–2761.
- (34) Orsi, M.; Haubertin, D. Y.; Sanderson, W. E.; Essex, J. W. *J. Phys. Chem. B* **2008**, *112*, 802–815.
- (35) Liu, Y.; Ichijo, T. *J. Phys. Chem.* **1996**, *100*, 2723–2730.
- (36) Yesylevskyy, S. O.; Schäfer, L. V.; Sengupta, D.; Marrink, S. J. *PLoS Comput. Biol.* **2010**, *6*, e1000810.
- (37) Singh, G.; Tieleman, D. P. *J. Chem. Theory Comput.* **2011**, *7*, 2316–2324.
- (38) Vorobyov, I.; Bekker, B.; Allen, T. W. *Biophys. J.* **2010**, *98*, 2904–2913.
- (39) Darre, L.; Machado, M. R.; Dans, P. D.; Herrera, F. E.; Pantano, S. *J. Chem. Theory Comput.* **2010**, *6*, 3793–3807.
- (40) Riniker, S.; van Gunsteren, W. F. *J. Chem. Phys.* **2011**, *134*, 084110.
- (41) Wu, Z.; Cui, Q.; Yethiraj, A. *J. Phys. Chem. B* **2010**, *114*, 10524–10529.
- (42) Wu, Z.; Cui, Q.; Yethiraj, A. *J. Phys. Chem. Lett.* **2011**, *2*, 1794–1798.
- (43) MacCallum, J. L.; Moghaddam, M. S.; Chan, H. S.; Tieleman, D. P. *Proc. Natl. Acad. Sci. U.S.A.* **2007**, *104*, 6206–6210.
- (44) Berne, B. J.; Weeks, J. D.; Zhou, R. H. *Annu. Rev. Phys. Chem.* **2009**, *60*, 85–103.

- (45) Shinoda, W.; Devane, R.; Klein, M. L. *Mol. Simul.* **2007**, *33*, 27–36.
- (46) Fumi, F. G.; Tosi, M. P. *J. Phys. Chem. Solids* **1964**, *25*, 31–43.
- (47) Fumi, F. G.; Tosi, M. P. *J. Phys. Chem. Solids* **1964**, *25*, 45–52.
- (48) MacCallum, J. L.; Bennett, W. F. B.; Tielemans, D. P. *Biophys. J.* **2008**, *94*, 3393–3404.
- (49) Baron, R.; de Vries, A. H.; Hünenerger, P. H.; van Gunsteren, W. F. *J. Phys. Chem. B* **2006**, *110*, 8464–8473.
- (50) Alemani, D.; Collu, F.; Casella, M.; Peraro, M. D. *J. Chem. Theory Comput.* **2010**, *6*, 315–324.
- (51) Hess, B.; Kutzner, C.; van der Spoel, D.; Lindahl, E. *J. Chem. Theory Comput.* **2008**, *4*, 435–447.
- (52) Berendsen, H. J. C.; Postma, J. P. M.; van Gunsteren, W. F.; Dinola, A.; Haak, J. R. *J. Chem. Phys.* **1984**, *81*, 3684–3690.
- (53) Miyamoto, S.; Kollman, P. A. *J. Comput. Chem.* **1992**, *13*, 952–962.
- (54) Hess, B.; Bekker, H.; Berendsen, H. J. C.; Fraaije, J. G. E. M. *J. Comput. Chem.* **1997**, *18*, 1463–1472.
- (55) Beveridge, D. L.; DiCapua, F. M. *Annu. Rev. Biophys. Biophys. Chem.* **1989**, *18*, 431–492.
- (56) van Gunsteren, W. F.; Daura, X.; Mark, A. E. *Helv. Chim. Acta* **2002**, *85*, 3113–3129.
- (57) Venable, R. M.; Skibinsky, A.; Pastor, R. W. *Mol. Simul.* **2006**, *32*, 849–855.
- (58) Jiang, F. Y.; Bouret, Y.; Kindt, J. T. *Biophys. J.* **2004**, *87*, 182–192.
- (59) Humphrey, W.; Dalke, A.; Schulten, K. *J. Mol. Graphics* **1996**, *14*, 1, 33–38.
- (60) Yu, H.; Karplus, M. *J. Chem. Phys.* **1988**, *89*, 2366.
- (61) Baron, R.; Trzesniak, D.; de Vries, A. H.; Elsener, A.; Marrink, S. J.; van Gunsteren, W. F. *Chem. Phys. Chem.* **2007**, *8*, 452–461.
- (62) Khadikar, P. V.; Mandloi, D.; Bajaj, A. V.; Joshi, S. *Bioorg. Med. Chem. Lett.* **2003**, *13*, 419–422.
- (63) Nagle, J. F.; Tristram-Nagle, S. *Biochim. Biophys. Acta* **2000**, *1469*, 159–195.
- (64) Kučerka, N.; Nagle, J. F.; Sachs, J. N.; Feller, S. E.; Pencer, J.; Jackson, A.; Katsaras, J. *Biophys. J.* **2008**, *95*, 2356–2367.
- (65) Balgavý, P.; Dubnicková, M.; Kučerka, N.; Kiselev, M. A.; Yaradaikin, S. P.; Uhríková, D. *Biochim. Biophys. Acta* **2001**, *1*, 40–52.
- (66) Petrache, H. I.; Dodd, S.; Brown, M. *Biophys. J.* **2000**, *79*, 3172–3192.
- (67) Rand, R. P.; Parsegian, V. A. *Biochim. Biophys. Acta* **1989**, *988*, 351–376.
- (68) Petrache, H. I.; Stephanie, T. N.; Gawrisch, K.; Harries, D.; Parsegian, V. A.; Nagle, J. F. *Biophys. J.* **2004**, *86*, 1574–1586.
- (69) Rawicz, W.; Olbrich, K. C.; McIntosh, T.; Needham, D.; Evans, E. *Biophys. J.* **2000**, *79*, 328–339.
- (70) Genco, I.; Gliozi, A.; Relini, A.; Robello, M.; Scallas, E. *Biophys. J.* **1993**, *1149*, 10–18.
- (71) Zhelev, D.; Needham, D. *Biochim. Biophys. Acta* **1993**, *1147*, 89–104.
- (72) Moroz, J. D.; Nelson, P. *Biophys. J.* **1997**, *72*, 2211–2216.
- (73) de Joannis, J.; Jiang, F. Y.; Kindt, J. T. *Langmuir* **2006**, *22*, 998–1005.
- (74) Glaser, R. W.; Leikin, S. L.; Chernomordik, L. V.; Pastushenko, V. F.; Sokirk, A. I. *Biochim. Biophys. Acta* **1988**, *940*, 275–287.
- (75) Kuo, A.-L.; Wade, C. G. *Biochemistry* **1979**, *18*, 2300–2308.
- (76) Rand, R. P.; Fuller, N. L. *Biophys. J.* **1994**, *66*, 2127–2138.
- (77) Zimmerberg, J.; Kozlov, M. M. *Nat. Rev. Mol. Cell Biol.* **2006**, *7*, 9–19.
- (78) Kirk, G. L.; Gruner, S. M.; Stein, D. L. *Biochemistry* **1984**, *23*, 1093–1102.
- (79) Gruner, S. M. *Proc. Natl. Acad. Sci. U.S.A.* **1985**, *82*, 3665–3669.
- (80) Turner, D. C.; Gruner, S. M. *Biochemistry* **1992**, *31*, 1340–1355.
- (81) Li, L.; Vorobyov, I.; Allen, T. W. *J. Phys. Chem. B* **2008**, *112*, 9574–9587.
- (82) Herce, H. D.; Garcia, A. E. *Proc. Natl. Acad. Sci. U.S.A.* **2007**, *104*, 20805–20810.
- (83) Lee, H. L.; Dubikovskaya, E. A.; Hwang, H.; Semyonov, A. N.; Wang, H.; Jones, L. R.; Twieg, R. J.; Moerner, W. E.; Wender, P. A. *J. Am. Chem. Soc.* **2008**, *130*, 9364–9370.
- (84) Yesylevskyy, S.; Marrink, S. J.; Mark, A. E. *Biophys. J.* **2009**, *97*, 40–49.
- (85) Schmidt, N.; Mishra, A.; Lai, G. H.; Wong, G. C. L. *FEBS Lett.* **2010**, *584*, 1806–1813.
- (86) Schmidt, N. W.; Mishra, A.; Lai, G. H.; Davis, M.; Sanders, L. K.; Tran, D.; Garcia, A.; Tai, K. P.; McCray, P. B., Jr.; Ouellette, A. J.; Selsted, M. E.; Wong, G. C. L. *J. Am. Chem. Soc.* **2011**, *133*, 6720–6727.
- (87) Gurtovenko, A. A.; Vattulainen, I. *J. Am. Chem. Soc.* **2005**, *127*, 17570–17571.
- (88) Gurtovenko, A. A.; Vattulainen, I. *Biophys. J.* **2007**, *92*, 1878–1890.
- (89) Praprotnik, M.; Matysiak, S.; Site, L. D.; Kremer, K.; Clementi, C. *J. Phys.: Condens. Matter* **2007**, *19*, 292201.
- (90) Matysiak, S.; Clementi, C.; Praprotnik, M.; Kremer, K.; Site, L. D. *J. Chem. Phys.* **2008**, *128*, 024503.